INTERNATIONAL JOURNAL FOR NUMERICAL METHODS IN FLUIDS, VOL. 16, 845–854 (1993)

NUMERICAL SOLUTION OF AXISYMMETRIC CAVITY FLOWS USING THE BOUNDARY ELEMENT METHOD

L. C. WROBEL

Wessex Institute of Technology, University of Portsmouth, Ashurst Lodge, Ashurst, Southampton SO4 2AA, U.K.

SUMMARY

This paper presents a formulation of the boundary element method (BEM) for solution of axisymmetric cavity flow problems. The governing equation is written in terms of Stokes' stream function, requiring a new fundamental solution to be found. The iterative procedure for adjusting the free-surface position is similar to that used for planar cavity flows. Numerical results are compared with finite difference and finite element solutions, showing the robustness of the BEM model.

KEY WORDS Boundary element method Cavity flow Riabouchinsky flow Free surface flow

INTRODUCTION

This paper presents an extension, for axially symmetric problems, of a recently developed BEM algorithm for planar cavity flows.[1] The basic assumptions are that of potential flow past a disk, placed perpendicular to the flow direction, in a channel of finite width and infinite length. Immediately behind the disk a cavity is formed containing air at a constant pressure; the primary objective of the study is to find the shape and size of this cavity.

The closure model adopted, proposed by Riabouchinsky,[2] assumes that an image disk can be placed in the flow at some point downstream from the original disk and that the flow geometry will be symmetric about the line midway between the disks (Figure 1). Owing to the axial symmetry of the flow, only one-quarter of the region in Figure 1 needs to be considered in the numerical analysis (Figure 2).

For two-dimensional problems, the governing equation for both the velocity potential and stream function is Laplace's equation. For axisymmetric problems, however, while the governing equation for the velocity potential is also Laplace's, the same is not true for the Stokes' stream function. Because the iteration algorithm to determine the free-surface position is better suited to a stream function scheme, an appropriate BEM formulation had to be developed. This required the derivation of an integral equation through a reciprocal theorem, and finding a fundamental solution specific to the problem.

The iteration algorithm for determining the free-surface position is similar to that of Reference 1. No special consideration is given to the singularity at the separation point, which was accounted for by local refinement. Numerical results are compared with available finite difference (FDM)[3] and finite element (FEM)[4] solutions.

0271–2091/93/090845–10$10.00

Received June 1992
Revised December 1992

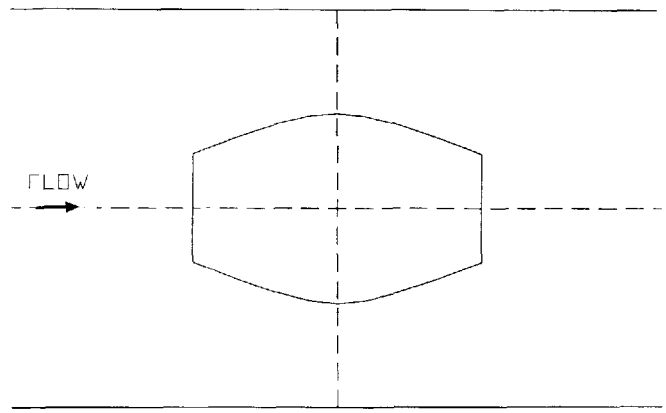

Figure 1. Riabouchinsky cavity model

FORMULATION OF THE PROBLEM

A sketch of the Riabouchinsky cavity model adopted in this work can be seen in Figure 2. The computational region is truncated at a certain distance upstream, where the flow is assumed to be parallel to the channel walls.

For the steady, irrotational, axisymmetric flow of an incompressible, inviscid fluid the following equations apply using cylindrical co-ordinates (x, r):

$$\frac{\partial u}{\partial x}+\frac{1}{r}v+\frac{\partial v}{\partial r}=0 \qquad \text{(continuity)}, \tag{1}$$

$$\frac{\partial u}{\partial r}-\frac{\partial v}{\partial x}=0 \qquad \text{(irrotationality)}, \tag{2}$$

$$p+\tfrac{1}{2}\rho q^2+\rho g r=\beta \qquad \text{(Bernoulli)}, \tag{3}$$

in which u, v are the velocity components in directions x and r, respectively, $q=(u^2+v^2)^{1/2}$ is the velocity magnitude, p is the pressure, ρ is the fluid density, g the acceleration due to gravity and β is Bernoulli's constant.

Introducing the Stokes' stream function ψ such that

$$u=\frac{1}{r}\frac{\partial \psi}{\partial r}, \qquad v=-\frac{1}{r}\frac{\partial \psi}{\partial x}$$

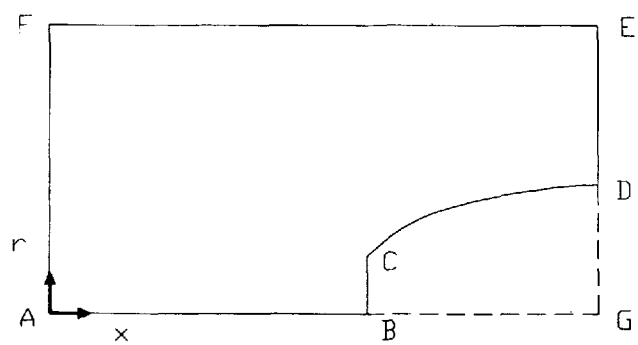

Figure 2. Definition of problem region

and substituting into (1) and (2), one notes that the continuity equation is identically satisfied and the irrotationality condition gives rise to the equation

$$\frac{\partial^2\psi}{\partial r^2}-\frac{1}{r}\frac{\partial\psi}{\partial r}+\frac{\partial^2\psi}{\partial x^2}=0. \tag{4}$$

The boundary conditions of the problem are as follows, referring to Figure 2: line ABCD is a streamline and, without loss of generality, its value can be set to $\psi=0$. The channel wall, line EF, is also a streamline with value $\psi=\psi_H=q_0H^2/2$, in which q_0 is the onset velocity magnitude and H the channel radius. Line DE is a symmetry axis; so, $\partial\psi/\partial x=0$ can be applied. At the truncating boundary AF the velocity field is parallel to the channel wall; thus, it is possible to apply either $\psi=q_0r^2/2$ or $\partial\psi/\partial x=0$.

The problem is solved by assuming an initial guess for the free-surface position and using Bernoulli's equation to correct it during an iteration process. It is customary to assume that the hydrostatic pressure is approximately uniform over the region of interest and to neglect the effects of gravity; as a consequence of (3), the fluid velocity is uniform in magnitude on the free streamline. This is an accurate assumption when $gr\ll q^2$, which holds true in this case.[5]

Denoting quantities referenced to the cavity or free streamline by the subscript c, we may write from (3)

$$p_e+\tfrac{1}{2}\rho q^2=\tfrac{1}{2}\rho q_c^2=\beta, \tag{5}$$

in which $p_e=p-p_c$ and the constant value of the pressure p_c has been incorporated into β. This expression permits computing the pressure at any point once the velocity field has been determined.

An important parameter in cavity flows is the Prandtl cavitation number σ, defined by

$$\sigma=\frac{q_c^2}{q_0^2}-1.$$

The problem can be made non-dimensional by putting

$$x^*=x/H,\quad r^*=r/H,\quad \psi^*=\psi/\psi_H,\quad q^*=2q/q_0.$$

The mathematical problem to be solved is then described by the following equations (dropping the asterisks for simplicity):

$$\frac{\partial^2\psi}{\partial r^2}-\frac{1}{r}\frac{\partial\psi}{\partial r}+\frac{\partial^2\psi}{\partial x^2}=0 \quad \text{in ABCDEFA}, \tag{6}$$

$$\psi=0 \qquad \text{on AB, BC, CD}, \tag{7}$$

$$\frac{\partial\psi}{\partial x}=0 \qquad \text{on DE}, \tag{8}$$

$$\psi=1 \qquad \text{on EF}, \tag{9}$$

$$\frac{\partial\psi}{\partial x}=0 \qquad \text{on AF}, \tag{10}$$

$$\frac{1}{r}\frac{\partial\psi}{\partial n}=-q_c \qquad \text{on CD}, \tag{11}$$

with the cavitation number given by

$$\sigma=\frac{q_c^2}{4}-1.$$

It is noted that the value of q_c is to be determined as part of the solution of the problem, together with the location of the free surface CD.

BOUNDARY INTEGRAL EQUATION

The first step in the BEM formulation is to obtain a boundary integral equation equivalent to equation (6). In the present case, we start from the reciprocal theorem:

$$\int_\Gamma \left(\frac{1}{r}\frac{\partial \psi}{\partial n}\psi^* - \frac{1}{r}\frac{\partial \psi^*}{\partial n}\psi \right) d\Gamma = 0, \tag{12}$$

which is valid in a region Ω bounded by the contour Γ. In the above expression, ψ and ψ^* are any two regular solutions of equation (6).

The above theorem can be proved as follows:

$$\begin{aligned}
\int_\Gamma \frac{1}{r}\frac{\partial \psi}{\partial n}\psi^* d\Gamma &= \int_\Gamma \frac{1}{r}\left(\frac{\partial \psi}{\partial r}n_r + \frac{\partial \psi}{\partial x}n_x \right)\psi^* \, d\Gamma \\
&= \int_\Gamma \left[\left(\frac{1}{r}\frac{\partial \psi}{\partial r}\psi^* \right)n_r + \left(\frac{1}{r}\frac{\partial \psi}{\partial x}\psi^* \right)n_x \right] d\Gamma \\
&= \int_\Omega \left[\frac{\partial}{\partial r}\left(\frac{1}{r}\frac{\partial \psi}{\partial r}\psi^* \right) + \frac{\partial}{\partial x}\left(\frac{1}{r}\frac{\partial \psi}{\partial x}\psi^* \right) \right] d\Omega \\
&= \int_\Omega \left[\frac{\partial}{\partial r}\left(\frac{1}{r}\frac{\partial \psi}{\partial r} \right) + \frac{\partial}{\partial x}\left(\frac{1}{r}\frac{\partial \psi}{\partial x} \right) \right]\psi^* \, d\Omega + \int_\Omega \left(\frac{1}{r}\frac{\partial \psi}{\partial r}\frac{\partial \psi^*}{\partial r} + \frac{1}{r}\frac{\partial \psi}{\partial x}\frac{\partial \psi^*}{\partial x} \right) d\Omega \\
&= \int_\Omega \frac{1}{r}\left(\frac{\partial^2 \psi}{\partial r^2} - \frac{1}{r}\frac{\partial \psi}{\partial r} + \frac{\partial^2 \psi}{\partial x^2} \right)\psi^* \, d\Omega + \int_\Omega \left(\frac{1}{r}\frac{\partial \psi}{\partial r}\frac{\partial \psi^*}{\partial r} + \frac{1}{r}\frac{\partial \psi}{\partial x}\frac{\partial \psi^*}{\partial x} \right) d\Omega.
\end{aligned}$$

Since the expression between brackets in the first integral is zero (equation (6)), the final result is

$$\int_\Gamma \frac{1}{r}\frac{\partial \psi}{\partial n}\psi^* \, d\Gamma = \int_\Omega \left(\frac{1}{r}\frac{\partial \psi}{\partial r}\frac{\partial \psi^*}{\partial r} + \frac{1}{r}\frac{\partial \psi}{\partial x}\frac{\partial \psi^*}{\partial x} \right) d\Omega. \tag{13}$$

In a similar manner, it is possible to show that

$$\int_\Gamma \frac{1}{r}\frac{\partial \psi^*}{\partial n}\psi \, d\Gamma = \int_\Omega \left(\frac{1}{r}\frac{\partial \psi^*}{\partial r}\frac{\partial \psi}{\partial r} + \frac{1}{r}\frac{\partial \psi^*}{\partial x}\frac{\partial \psi}{\partial x} \right) d\Omega. \tag{14}$$

The theorem is then proved by subtracting (14) from (13).

The next step in the formulation is to consider that ψ is the required solution of the boundary-value problem and ψ^* is the fundamental solution of equation (6), given by[6]

$$\psi^* = \frac{1}{(a+b)^{1/2}}[aK - (a+b)E], \tag{15}$$

where

$$\begin{aligned}
a &= r^2(\xi) + r^2(\chi) + [x(\xi) - x(\chi)]^2, \\
b &= 2r(\xi)r(\chi),
\end{aligned}$$

in which ξ and χ are the source and field points, and $K = K(m)$ and $E = E(m)$ are the complete elliptic integrals of the first and second kind, respectively, with parameter $m = 2b/(a+b)$. The

derivative of ψ^* with respect to the normal is of the form

$$\frac{\partial\psi^*}{\partial n}=\frac{x(\chi)-x(\xi)}{(a+b)^{1/2}}\left(K-\frac{a}{a-b}E\right)n_x+\frac{r(\chi)}{(a+b)^{1/2}}\left[K+\frac{2r^2(\xi)-a}{a-b}E\right]n_r. \tag{16}$$

The fundamental solution ψ^* presents a discrete, weak singularity when the source and field points are coincident, for in this case $a=b$, $m=1$ and $E(m)=1$, $K(m)\sim\ln(1-m)\to-\infty$.[7] Hence, for the reciprocal theorem (12) to be valid with ψ^* given by (15), it is necessary to exclude the source point ξ by surrounding it with a small circle of radius ε centred at the source point, in the form

$$\int_{\Gamma+\Gamma_\varepsilon}\left(\frac{1}{r}\frac{\partial\psi}{\partial n}\psi^*-\frac{1}{r}\frac{\partial\psi^*}{\partial n}\psi\right)\mathrm{d}\Gamma=0. \tag{17}$$

Taking the limit as $\varepsilon\to0$, the following results are obtained:

$$\lim_{\varepsilon\to0}\int_{\Gamma_\varepsilon}\frac{1}{r(\chi)}\frac{\partial\psi(\chi)}{\partial n(\chi)}\psi^*(\xi,\chi)\,\mathrm{d}\Gamma(\chi)=0,$$

$$\lim_{\varepsilon\to0}\int_{\Gamma_\varepsilon}\frac{1}{r(\chi)}\frac{\partial\psi^*(\xi,\chi)}{\partial n(\chi)}\psi(\chi)\,\mathrm{d}\Gamma(\chi)=\psi(\xi).$$

Thus, equation (17) takes the form

$$\psi(\xi)+\int_\Gamma\frac{1}{r(\chi)}\frac{\partial\psi^*(\xi,\chi)}{\partial n(\chi)}\psi(\chi)\,\mathrm{d}\Gamma(\chi)=\int_\Gamma\frac{1}{r(\chi)}\frac{\partial\psi(\chi)}{\partial n(\chi)}\psi^*(\xi,\chi)\,\mathrm{d}\Gamma(\chi). \tag{18}$$

If the source point ξ is a boundary point, the above equation is modified as follows:

$$c(\xi)\psi(\xi)+\int_\Gamma\frac{1}{r(\chi)}\frac{\partial\psi^*(\xi,\chi)}{\partial n(\chi)}\psi(\chi)\,\mathrm{d}\Gamma(\chi)=\int_\Gamma\frac{1}{r(\chi)}\frac{\partial\psi(\chi)}{\partial n(\chi)}\psi^*(\xi,\chi)\,\mathrm{d}\Gamma(\chi). \tag{19}$$

in which $c(\xi)$ is a geometric coefficient dependent on the location of the source point.[8]

It is interesting to note that, for a point on the axis of revolution (i.e. $r(\xi)=0$ or $r(\chi)=0$), we have $b=0$, $m=0$, $E=K=\pi/2$. These values lead to ψ^* and $\partial\psi^*/\partial n$ both being equal to zero. Thus, there is no need to include the rotational symmetry axis AB in the numerical analysis, which is consistent with the BEM formulation of axisymmetric problems.[8]

NUMERICAL SOLUTION

For the numerical solution of the problem, the boundary Γ (the generating contour BCDEFA in Figure 2) is subdivided into a number of straight elements. Linear interpolation functions are then introduced to relate the variation of the functions within each element to their values at the nodal (extreme) points.

The variables considered in this work were ψ and $q=(1/r)(\partial\psi/\partial n)$; it is also possible to consider $\partial\psi/\partial n$ as a variable and calculate q '*a posteriori*', but the difference in the numerical results is negligible.

The symmetry axis DE was taken into account by reflection and condensation as discussed by Brebbia *et al.*[8] This is similar to considering image sources, and avoids the discretization of the symmetry axis. Thus, the discretized version of equation (19) becomes

$$c(\xi)\psi(\xi)+\sum_{j=1}^{M}\int_{\Gamma_j}q^*(\xi,\chi)(N_1\psi_1+N_2\psi_2)\,\mathrm{d}\Gamma(\chi)=\sum_{j=1}^{M}\int_{\Gamma_j}\psi^*(\xi,\chi)(N_1q_1+N_2q_2)\,\mathrm{d}\Gamma(\chi), \tag{20}$$

in which M represents the number of boundary elements along the lines BCD and EFA, $q^*(\xi, \chi)=(1/r(\chi))(\partial\psi^*(\xi, \chi)/\partial n(\chi))$, N_1 and N_2 are linear interpolation functions, and ψ_1, q_1, ψ_2, q_2 represent nodal values of each element.

Equation (20) can be written in assembled form as follows:

$$c_i\psi_i+\sum_{j=1}^{M} H_{ij}\psi_j=\sum_{j=1}^{M} G_{ij}q_j, \tag{21}$$

where the subscript i stands for values at the source point. The above equation relates the value of ψ at the source point to M boundary values of ψ and q, half of which are prescribed as boundary conditions. Since equation (21) is valid at any boundary point, we apply it, using a collocation technique, to the M nodal points of the discretization, generating a system of algebraic equations which is formally written as

$$\mathbf{H}\boldsymbol{\psi}=\mathbf{G}\mathbf{q}. \tag{22}$$

Introducing boundary conditions (7) along lines BC and CD, (9) on EF and (10) on FA, and reordering (22), the final system can be solved by using a standard technique such as Gauss elimination.

The coefficients of matrices **H** and **G** are the result of integrations over boundary elements. The off-diagonal coefficients involve the evaluation of regular integrals; this is done by using a standard Gauss quadrature, with the number of integration points determined as a function of the distance between source point and element under consideration.

The diagonal coefficients of both matrices require the evaluation of singular integrals. For the coefficients G_{ii}, the singularity is logarithmic and the corresponding integrals are calculated using an adaptive Gauss quadrature scheme developed by Telles.[9] On the other hand, the coefficients H_{ii} involve not only logarithmic singular integrals but also stronger ones, which have to be computed in the Cauchy principal value sense. For them, a modification of Telles' scheme proposed by Cerrolaza and Alarcon[10] is employed.

ITERATION ALGORITHM

For the numerical solution of the problem, an initial free-surface location is assumed. The BEM solution then produces the value of q_c at each point along the free surface. These values are all equal for the correct free-surface position (but, of course, not for the assumed one), and it is essential that a procedure be devised to properly move the free surface in the steps of the iteration scheme so that the constant-velocity condition be more closely satisfied on the moved streamline.

With the objective of obtaining a relation between increments of q_c and r on the free-surface points, we define $\bar{q}$ as the average velocity in a vertical section of the flow. Thus, the flow rate Q can be expressed as

$$Q=\bar{q}\pi(H^2-r^2) \tag{23}$$

or, in non-dimensional form,

$$\bar{q}(1-r^2)=1. \tag{24}$$

The next step is to derive an approximate relation between $\bar{q}$ and q_c. It is noted that, in the region behind the disk, $\bar{q}(x)$ should increase with x and be lower than the free-surface velocity q_c. The following empirical relation was then adopted, similarly to Reference 1,

$$\bar{q}=q_c\frac{r}{1-r^2}, \tag{25}$$

which complies with the previous requirements. Substituting in expression (24), we obtain

$$q_c r = 1 \quad \text{or} \quad q_c = \frac{1}{r}. \tag{26}$$

The iteration procedure will then be as follows:

(i) Assume an initial free-surface location.
(ii) BEM solution provides q_c along the free surface.
(iii) Calculate β at each free surface node i, i.e.

$$\beta_i = \tfrac{1}{2}\rho q_{ci}^2. \tag{27}$$

(iv) Calculate $\Delta\beta_i = \beta_C - \beta_i$, in which β_C is the value of β at point C, the separation point. This value was selected because point C, the disk tip, is a fixed free-surface point.
(v) Calculate Δr_i by substituting (26) into (27) to obtain

$$\beta_i = \frac{\rho}{2r_i^2}, \tag{28}$$

$$\frac{\Delta\beta}{\Delta r} \approx \frac{\mathrm{d}\beta}{\mathrm{d}r} = -\frac{\rho}{r_i^3}, \tag{29}$$

$$\Delta r_i = -\frac{\Delta\beta_i r_i^3}{\rho}. \tag{30}$$

(vi) Compute the relative norm of increments

$$\frac{1}{M_f}\sum_{i=1}^{M_f}\left|\frac{\Delta r_i^{k+1}}{r_i^k}\right|, \tag{31}$$

where M_f is the number of free-surface nodes. If the norm is smaller than a specified tolerance ε, the process has converged and is terminated; otherwise, the free surface is moved to a new location given by $r_i^{k+1} = r_i^k + \omega\,\Delta r_i^{k+1}$, with ω a relaxation parameter, and the process returns to step (ii).

RESULTS OF ANALYSES

Some results are now presented concerning the problem depicted in Figure 2. For simplicity, we call $\overline{BC} = d$, $\overline{BG} = L$, $\overline{DG} = b$ and $\overline{AB} = a$.

For specified values of a and d, the problem contains three free parameters, i.e. L, b and q_c, and one more needs to be prescribed to define the problem fully. As pointed out by Aitchison,[4] the natural choice from the physical point of view is to fix q_c, which is equivalent to specifying the pressure far upstream. However, small changes in the pressure lead to large changes in the cavity length, and the problem becomes more difficult from the mathematical point of view. Thus, it is preferable to fix the length L and compute b and q_c as part of the solution.

Results are presented in Table I for $d = 0{\cdot}25$, $L = 1{\cdot}0$. These results were obtained using two different initial guesses for the free surface: the straight line $r = d$ and a quarter of an ellipse with the centre along the line $\overline{EG}$ at $r = d$, and semi-axes L and 0·15. Also presented are the FEM solution of Aitchison[4] and the FDM one of Brennen.[3]

The results of Brennen[3] were given in graphical form, and the FDM values quoted in Table I have been extrapolated from these graphs. The FDM formulation employed a transformed

Table I. Results for $d=0{\cdot}25$, $L=1{\cdot}0$

Method	b	σ
BEM	0·455	0·690
FEM	0·412	0·548
FDM	0·44	0·66

(ϕ, ψ)-plane (ϕ being a velocity potential) where the flow region becomes rectangular. The problem solution required a graded mesh, point-by-point Gauss–Seidel iteration, over-relaxation, a special treatment of the singularity and the optimization of some parameters to obtain a stable and convergent scheme. Brennen[3] also performed experimental tests in a water tunnel which confirmed the accuracy of his numerical results. The FEM procedure employed a refined moving mesh of linear triangular elements, computing the free surface position through a discrete minimization problem using a quasi-Newton method. This was solved repeatedly for different assumed values of q_c until the average pressure in all elements was positive.

The BEM discretization employed only 40 linear elements, with nine elements along the disk (line BC), 15 along the free surface (line CD), 12 along the channel wall (line EF) and four along the truncation boundary (line FA). The discretization was graded due to the singularity at the separation point C such that, along the free surface, the elements' lengths vary from around 0·0125 near point C to 0·2 near point D.

The BEM solution required a large number of iterations for a tolerance $\varepsilon=10^{-3}$, and a small value of the relaxation parameter $\omega=0{\cdot}05$ to control oscillations which predominantly appear in the first few iterations. The results, however, were insensitive to the initial free-surface position. The convergence pattern for the two different assumed positions is depicted in Figures 3 and 4. It

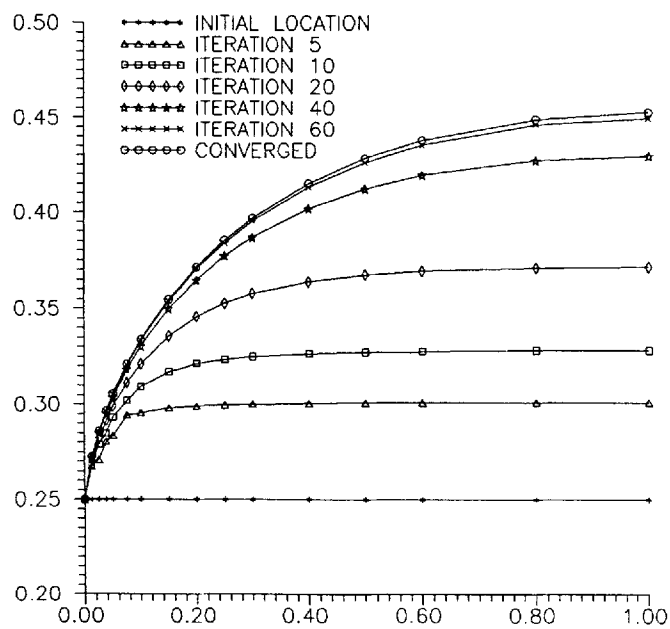

Figure 3. Convergence pattern for straight line as initial guess (distorted scale)

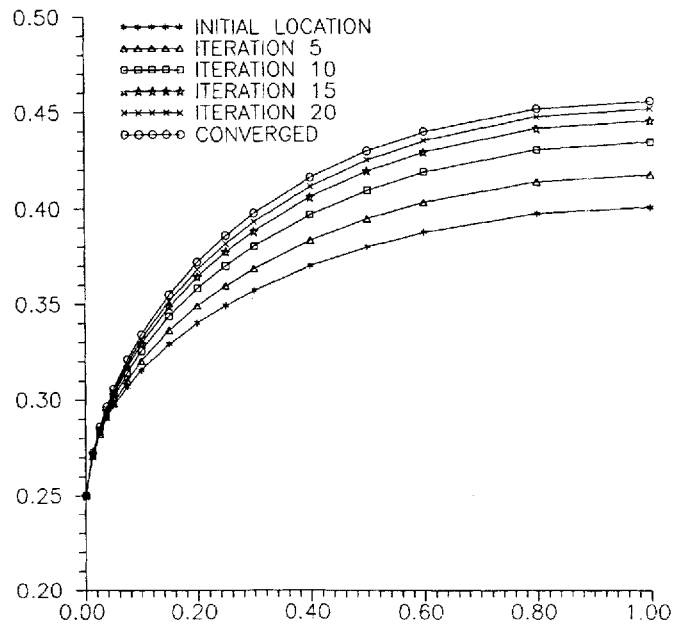

Figure 4. Convergence pattern for ellipse as initial guess (distorted scale)

can be seen that both cases converge to the same solution, and that the initial oscillations in Figure 3 were quickly dampened.

Tables II–IV depict the results obtained by the three methods for the cases of $d=0{\cdot}25$, $L=0{\cdot}5$; $d=0{\cdot}125$, $L=1{\cdot}0$; and $d=0{\cdot}125$, $L=0{\cdot}5$. Also included in Table III is the FDM result for σ obtained by Fox and Sankar[11] using the Regula–Falsi method, with no special considerations for the singularity at the separation point. All tables show the same pattern of results, with good agreement between the present BEM and FDM values interpolated or extrapolated from Brennen's graphs,[3] and with the FEM consistently predicting lower values.

Table II. Results for $d=0{\cdot}25$, $L=0{\cdot}5$

Method	b	σ
BEM	0·398	0·794
FEM	0·358	0·637
FDM	0·40	0·73

Table III. Results for $d=0{\cdot}125$, $L=1{\cdot}0$

Method	b	σ
BEM	0·296	0·288
FEM	0·250	0·209
FDM	0·29–0·30	0·28–0·29
R–F	—	0·113

Table IV. Results for $d=0{\cdot}125$, $L=0{\cdot}5$

Method	b	σ
BEM	0·245	0·375
FEM	0·203	0·275
FDM	0·24–0·25	0·34–0·35

Table V. Values of ψ along the truncation boundary FA for $d=0{\cdot}25$, $L=1{\cdot}0$, $q_0=2$

r	BEM	Exact
0·25	0·0623	0·0625
0·50	0·2495	0·25
0·75	0·5616	0·5625

It is interesting to point out that in all cases the truncation distance a was assumed equal to 2. The correctness of this assumption was verified from the calculated variation of ψ along the line FA, which agreed very well with the exact values (see Table V).

CONCLUSIONS

The BEM procedure for solving axisymmetric cavity flow problems described in the present paper has been shown to work well for a series of geometric configurations. The results obtained compare very favourably with the FDM ones of Brennen,[3] while the data preparation effort and computer time for the BEM are much smaller.

It may be possible to speed up the iteration process by considering a more realistic relationship between $\bar{q}$ and q_c than that given by expression (25), although several have been tested with no significant differences. It is noted, however, that any improvement will be in efficiency rather than in accuracy, since the algorithm already produces results which are accurate and insensitive to the initial position assumed for the free surface.

REFERENCES

1. L. C. Wrobel, 'A simple and efficient BEM algorithm for planar cavity flows', *Int. j. numer. methods fluids*, **14**, 529–537 (1992).
2. D. Riabouchinsky, 'On steady fluid motion with free surfaces', *Proc. Lond. Math. Soc.*, **19**, 206–215 (1920).
3. C. Brennen, 'A numerical solution of axisymmetric cavity flows', *J. Fluid Mech.*, **37**, 671–688 (1969).
4. J. M. Aitchison, 'The numerical solution of planar and axisymmetric cavitational flow problems', *Comput. Fluids*, **12**, 55–65 (1984).
5. G. K. Batchelor, *An Introduction to Fluid Dynamics*, Cambridge University Press, Cambridge, 1967.
6. G. Birkhoff and E. H. Zarantonello, *Jets, Wakes and Cavities*, Academic Press, New York, 1957.
7. M. Abramowitz and I. A. Stegun, *Handbook of Mathematical Functions*, Dover, New York, 1965.
8. C. A. Brebbia, J. C. F. Telles and L. C. Wrobel, *Boundary Element Techniques*, Springer, Berlin, 1984.
9. J. C. F. Telles, 'A self-adaptive coordinate transformation for efficient numerical evaluation of general boundary element integrals', *Int. j. numer. methods eng.*, **24**, 959–973, (1987).
10. M. Cerrolaza and E. Alarcon, 'A bi-cubic transformation for the numerical evaluation of the Cauchy principal value integrals in boundary methods', *Int. j. numer. methods eng.*, **28**, 987–999 (1989).
11. L. Fox and R. Sankar, 'The Regula–Falsi method for free boundary problems', *J. Inst. Maths. Applics.*, **12**, 49–54 (1973).